

Final Draft
of the original manuscript:

Meza Garcia, E.; Dobron, P.; Bohlen, J.; Letzig, D.; Chmelik, F.; Lukac, P.;
Kainer, K.U.:

**Deformation mechanisms in an AZ31 cast magnesium alloy as
investigated by the acoustic emission technique**

In: Materials Science and Engineering A (2006) Elsevier

DOI: 10.1016/j.msea.2006.02.469

**Deformation mechanisms in cast AZ31 magnesium alloy as investigated by the
acoustic emission technique**

Enrique Meza-García^{1*}, Patrik Dobroň², Jan Bohlen¹, Dietmar Letzig¹, František
Chmelík², Pavel Lukáč², Karl Ulrich Kainer¹

¹ GKSS-Research Centre, Institute for Materials Research, Centre for Magnesium
Technology, Max-Planck-Str. 1, D-21502 Geesthacht, Germany

² Department of Metal Physics, Charles University, Ke Karlovu 5, CZ 12116 Prague 2,
Czech Republic

* corresponding author, email: enrique.meza@gkss.de

Keywords: magnesium, alloy AZ31, acoustic emission, twinning

Abstract

Cast AZ31 magnesium alloy was deformed in tension and compression at temperatures between 25 – 350°C and at a constant strain rate of 10^{-3} s^{-1} . Measurements of the acoustic emission (AE) during testing are presented and related to the microstructure of the sample material. The AE count rates increase with increasing temperature from room temperature to a maximum at 230°C. At higher temperatures they decrease. This behaviour is discussed with a view to the role of twinning during deformation at elevated temperature.

Introduction

Due to the hexagonal close packed lattice structure of magnesium, basal slip is the main slip mode. It is important to note that it has only three geometrical and two independent slip systems and therefore non-basal slip as well as twinning have to be active. Basal slip, as well as prismatic slip systems, allow only slip along $\langle a \rangle$ -directions and this is not enough to satisfy the von Mises' yielding criterion for unrestricted plastic deformation. However, $\{10\bar{1}2\}$ twinning and $\{11\bar{2}2\} \langle 11\bar{2}3 \rangle$ ($\langle c + a \rangle$) pyramidal slip allow a contribution of deformation in direction of the $\langle c \rangle$ -axis. While $\langle c + a \rangle$ slip is only active at elevated temperature [1] twinning plays an important role during deformation at room temperature [2].

In the present experiments the relative contribution of twinning to the deformation of alloy AZ31 will be studied in tension and compression and at different temperatures using Acoustic Emission. AE stems from transient elastic waves, generated within a material due to sudden localised and irreversible structural changes. It responds e.g. to dislocations motion and twinning and therefore generates information on the dynamic processes involved in plastic deformation [3].

Experimental

A direct chill (DC) AZ31 cast billet has been homogenised (12 hr at 350°C) and is used for this study. Tensile (6 mm diameter, 60 mm length) and compression (10 mm diameter, 15 mm length) samples were cut with the main axis parallel to the cast direction. Tests were conducted at various temperatures from room temperature to 350 °C using a standard testing machine. A constant strain rate of 10^{-3} s^{-1} was applied.

Microstructural analysis by optical microscopy was carried out using longitudinal sections of the deformed samples after testing [4].

A computer controlled DAKEL-XEDO-3 AE system was used to monitor AE using two threshold-levels for detection, which yields a comprehensive set of AE parameters involving count rates \dot{N}_{C1} and \dot{N}_{C2} (count number per second [5]) at two threshold levels, giving total AE count and burst AE count by proper setting. The burst AE occurs mainly as a consequence of instable fashion of plastic deformation or degradation of materials as well as twinning. In order to avoid direct heating of the transducer during high temperature testing, a steel waveguide was attached to the tensile samples, to enable attaching the detector outside the furnace. In the case of compression tests the waveguide was attached to one of the dies which were in direct contact to the sample. This fact and different volumes and shapes of tensile and compression samples, however, prevent a quantitatively comparison of the count rates from tensile with those from compression tests.

Results

The engineering stress-strain curves and the corresponding AE count rates are shown in Figs. 1a - c for tensile and in Figs. 2a - d for compression tests at various temperature. In all cases an increase of the AE count rates up to a characteristic peak is observed near the macroscopic yield point, which is followed by a decrease. At room temperature this decrease is gradual in tension whereas in compression a faster drop is between 5 – 10 % strain. In both cases, tension and compression, this decrease shifts to higher strains as the temperature increases. Thus, the AE count rates generally increase up to 200°C and this is more pronounced in compression than in tension. Above this temperature they

decrease again earlier during the test. The integrated AE (total counts number) for both threshold levels (N_{C1} and N_{C2}) over a strain of 20% is shown in Fig. 3a for tensile and Fig. 3b for compression testing, respectively. The count number increases with the temperature to a maximum. Linear extrapolation of the two slopes in Fig. 3b gives a maximum at approximately 230°C. Fig. 4 shows the tensile and compression yield strength vs. temperature. As it can be expected, the yield strength decreases significantly with increasing temperature. Furthermore, for all temperatures there is only a small difference between tensile and compressive yield strength.

The microstructure of the specimens after testing consists of a large number of twins from room temperature up to 200°C (Figs. 5a and b). They begin to vanish when the temperature rises (Fig. 5c). Then also newly generated small grains located along the grain boundaries become visible as a “necklace” ring type [6]. This indicates the beginning of dynamic recrystallization (DRX).

Discussion

The small difference between tensile and compressive yield strength in Fig. 4 is interesting to note. A strong yield asymmetry is often observed in textured samples such as extruded bars [7]. This is in good correspondence with the results of Mann et al. [8]. Therefore, the processes that control the start of plastic deformation are likely to be the same in tension and compression, as expected from the random texture [9] of the material. However, the decrease in the AE count rates after the peak maximum is much more pronounced in compression than in tension (Figs. 1a and 2a) which reflects a much stronger effect of strain hardening. Note, that also the difference between yield strength and maximum strength is higher in compression than in tension.

Since important sources of AE are a massive dislocation multiplication and twinning, we can state that these AE sources are less active at higher strains. Massive dislocation motion is more and more hindered by forest dislocations as a result of strain hardening [3]. Twinning, however, lead to a re-orientation of grains and can contribute to the macroscopic strain as long as grains exist that are readily oriented for such a contribution. If these grains already twinned, no further twins can contribute to strain [10]. The kind of re-orientation is different in tension and compression due to a different direction of the applied stress.

Our microstructural analysis clearly states that twinning plays an important role as a deformation mechanism at temperatures between room temperature and 200 °C. Above 200°C, only some twins are still visible [11], which reflects that they do not play that important role anymore. Also the beginning of dynamic recrystallization is observed at this temperature [12].

Furthermore, above 200°C, the AE count number decreases. This is reasonable because the amount of twins (as important source of AE) decreases significantly with respect to the increase of temperature. This effect can be associated with the activation of additional deformation mechanisms [13] like prismatic $\langle a \rangle$ slip and, more important, second-order pyramidal $\langle c + a \rangle$ slip, because the CRSS (critical resolved shear stress) of these slip mode is strongly dependent on temperature [1]. While CRSS at room temperature for these slip modes is about 100 times larger than that for basal slip [14], it is rapidly decreasing with increasing temperature. We can understand that above 200°C the activation of non-basal slip system is more favourable than twinning. At this point it is worthwhile to repeat that $\langle c + a \rangle$ pyramidal slip is the only slip mode that contributes

to the macroscopic strain along the c-axis of the hcp – structure, as well as twinning does.

Both, the additional possibility to activate $\langle c + a \rangle$ slip as well as the beginning of dynamic recrystallisation do not contribute to the AE count rates. With a decreasing amount of twins, a decrease in the number of AE counts should occur.

From room temperature to 200°C a noteworthy increase of AE counts with respect to the temperature was found, with a peak at approximately 230°C (see Fig. 3b). As a matter of fact an increase in the AE count rates has to be associated with a massive dislocation glide and /or twinning. From a first point of view we would not assume that with increasing temperature an increase in massive dislocation motion occurs because a smoother type of dislocations glide is suggested. We cannot state on the role of twinning since a determination of the number of twins in micrographs was not achieved in the present experiments. Although we would not assume that more twins occur as a source of AE with increasing temperature, it has been shown by Yoshinaga et al. [15] that twins other than those with $\{10\text{-}12\}$ symmetry planes may occur, like those of $\{10\text{-}13\}$ or $\{30\text{-}34\}$ type. These twins may be better activated when the temperature increases to 100 or 200°C.

Although the reason for the increasing count rates cannot be structurally determined within the scope of this paper, we suggest an additional possibility in the view of these AE findings. As additional source for AE instable deformation mechanisms with a gradual tearing of dislocations from embedded atoms (Portevin – Le Chatelier effect) produce such a significant additional increase in the AE count rates [16]. If an additional instable interdependence between twinning and dislocation glide is assumed at elevated temperature this could also produce additional AE in terms of an “locking -

unlocking mechanism” of dislocations. In fact, as an indication for a general interdependence, an influence of twins on the strain hardening behaviour is reported [17]. Such simultaneous effect between twin development and dislocations mobility would also lead to an increase in the count rates, however, with twinning not occurring gradually. Therefore a steady increase with temperature would be assumed. If also recovery processes are enhanced with increasing temperature, strain hardening will be reduced so that mechanisms are active for a longer period of strain and measuring time.

Conclusions

Twinning plays an important role as a deformation mechanism in the range from room temperature up to 200°C which was observed in a microstructural analysis. Although a smoother deformation glide and a decrease in the activity of twinning would be assumed, AE count rates increase with temperature. Beside of a possible contribution of non- $\{10\text{-}12\}$ type twins with increasing temperature an instable interaction between twin formation, deformation glide and recovery is suggested, as it would also fit the AE findings of the present study.

Above 200°C dynamic recrystallization occurred and twins are not visible any more to that extent. A softening of the materials occurs. The AE count rates decrease again which is convenient with the start of dynamic recrystallization as well as other slip modes like $\langle c + a \rangle$ pyramidal slip being active.

Acknowledgements

This work is a part of the Research Project 1M 2560471601 "Eco-centre for Applied Research of Non-ferrous Metals" that is financed by the Ministry of Education, Youth

and Sports of the Czech Republic. It was also supported by the Grant Agency of the Academy of Sciences of the Czech Republic under grant A2112303.

References

- [1] S.E. Ion, F. J. Humphreys, S.H. White, *Acta Metall*, 30 (1982) 1909 – 1919.
- [2] U.F. Kocks, D.G. Westlake, *Trans. Metall. Soc.*, 239 (1967) 1107 - 1109.
- [3] C.R. Heiple, S.H. Carpenter, *J. Acoustic Emission* 6 (1987) 177 – 204.
- [4] V. Kree, J. Bohlen, D. Letzig, K.U. Kainer, *Pract. Metallogr.* 41 (2004) 233 - 246.
- [5] ASTM E 610-82, <http://www.appliedinspection.com/aeterms.htm>
- [6] L.W.F. MacKenzie, F.J. Humphreys, G.W. Lorimer, K. Savane, T. Wilks, in: K. U. Kaner ed., *Proc. 6th Int. Conf. Magnesium Alloys And Their Applications 2003*, Wiley-VCH Weinheim (2004) 158 – 163.
- [7] I.L. Dillamore, W.T. Roberts, *Metall Rev.* 1965; 10(39):271 – 328.
- [8] G. Mann, J. R. Griffiths, C. H. Cáceres, *J. Alloys Comp.* 378 (2004) 188-191.
- [9] J. Bohlen, S.B. Yi, J. Swiostek, D. Letzig, H. G. Brokmeier, K.U. Kainer, *Scripta Mater.* 53 (2005) 259 - 264.
- [10] C. H. J. Davies, S. Yi, J. Bohlen, K. U. Kainer, H.-G. Brokmeier, *Mater. Sci. Forum* 495 – 497 (2005) 1633 – 1638.
- [11] M.M. Myshlyaev, H.J. McQueen, A. Mwembela, E. Konopleva, *Mat. Sci. Eng. A337* (2000) 121 - 133.
- [12] O. Sitdikov, R. Kaibyshev, T. Sakai, *Mater. Sci. Forum* 419-422 (2003) 521-526.
- [13] K. Máthis, K. Nyilas, A. Axt, Dragomir-Cernatescu, T. Ungár, P. Lukác, *Acta Mater.* 52 (2004) 2889-2894.

- [14] M. H. Yoo, *Metal Trans A*, 12 (1981) 409 - 418.
- [15] H. Yoshinaga, T. Obara, S. Morozumi, *Mater. Sci. Eng.* 12 (1973) 255 - 264.
- [16] F. Chmelík, A. Ziegenbein, H. Neuhäuser, P. Lukáč, *Mater. Sci. Eng.* A324 (2002) 200 – 207.
- [17] M.R. Barnett, Z. Keshavarz, A.G. Beer, D. Atwell, *Acta Mater.* 52 (2004) 5093 – 5103.

Figure captions

Fig. 1. Stress-strain curve (broken line) and AE count rates \dot{N}_{C1} (solid line) \dot{N}_{C2} (dotted line) in tension test for AZ31 in cast direction at room temperature and constant strain rate of $1 \times 10^{-3} \text{ s}^{-1}$, at a) room temperature b) 200°C and c) 300°C.

Fig. 2. Stress-strain curve (broken line) and AE count rates \dot{N}_{C1} (solid line) \dot{N}_{C2} (dotted line) in compression test for AZ31 in cast direction at room temperature and constant strain rate of $1 \times 10^{-3} \text{ s}^{-1}$, at a) room temperature b) 100°C, c) 200°C and d) 300°C.

Fig. 3. AE counts from 0 to 20% strain for each threshold level (N_{C1} – solid squares - and N_{C2} – open circles-) in a) tension and b) compression in cast direction with a constant strain rate of $1 \times 10^{-3} \text{ s}^{-1}$ and different temperatures.

Fig. 4. Tensile (solid circles) and compressive yield strength (open circles) of cast AZ31 at various temperatures.

Fig. 5. Micrographs from longitudinal sections of the deformed samples after testing: a) room temperature, b) 200°C, c) 300°C

Fig 1a:

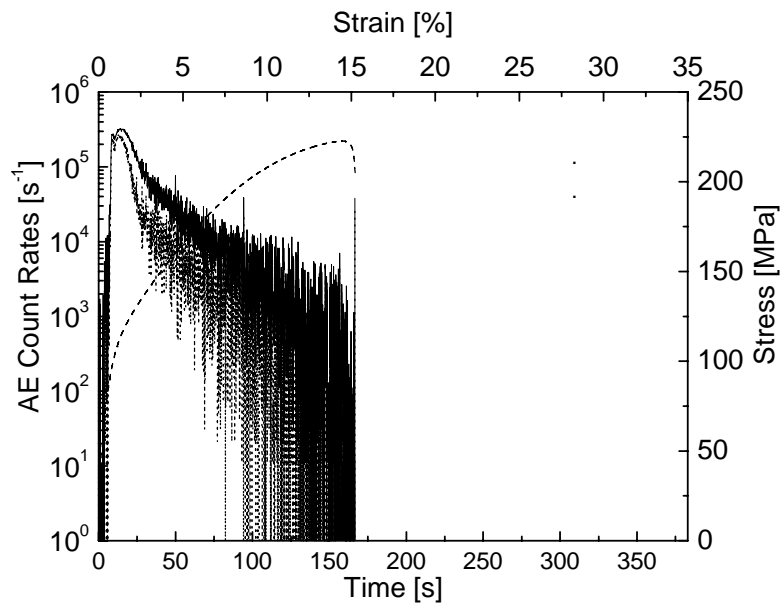


Fig 1b:

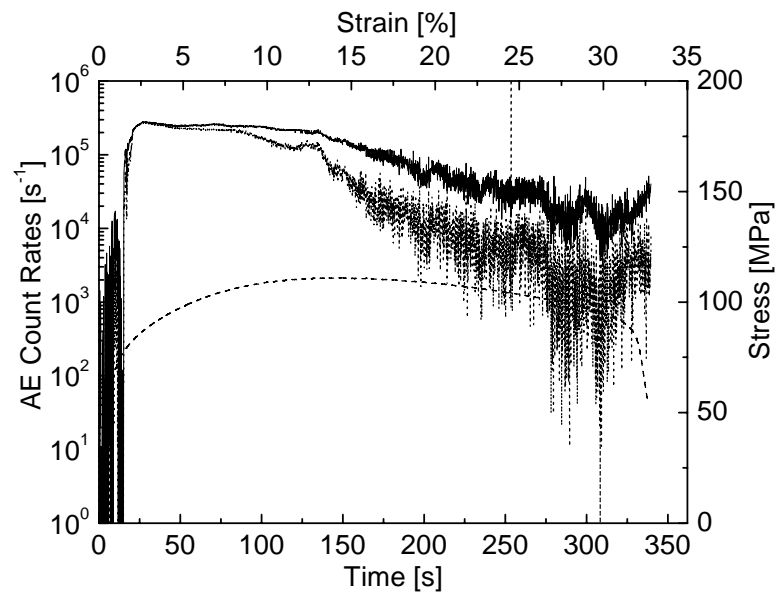


Fig 1c:

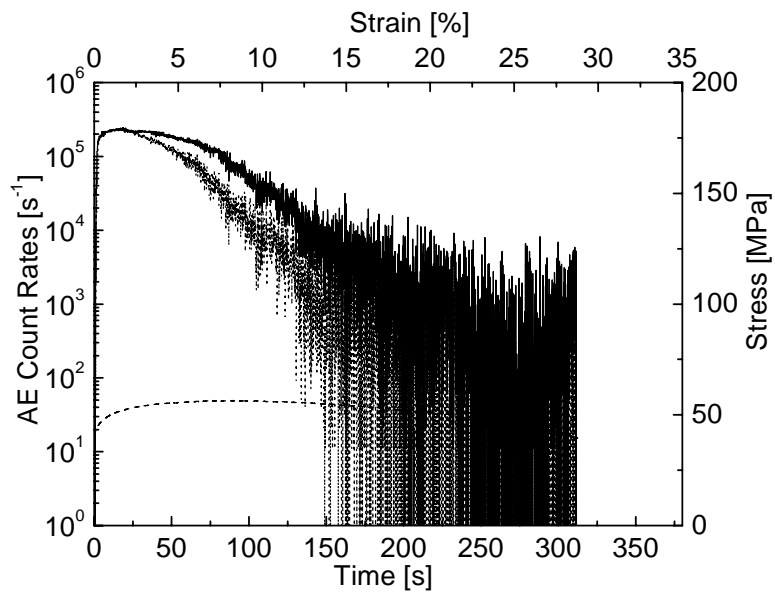


Fig 2a:

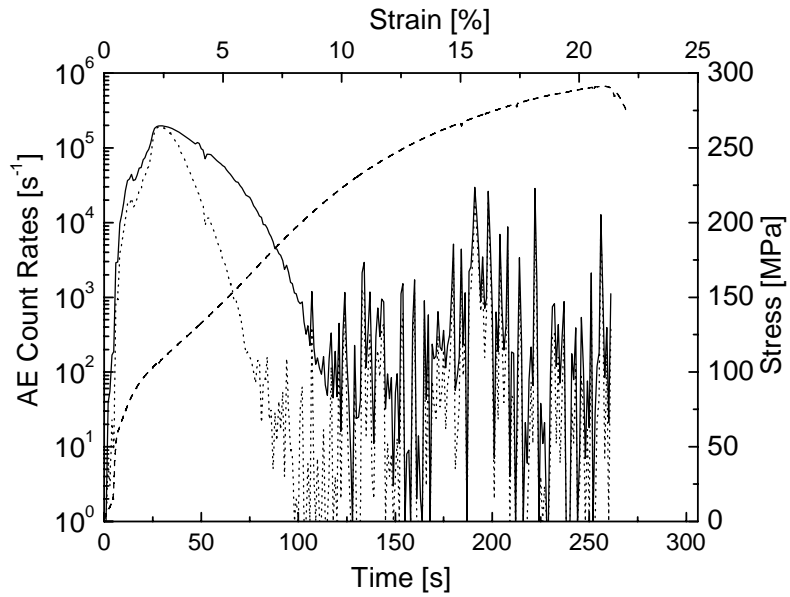


Fig 2b:

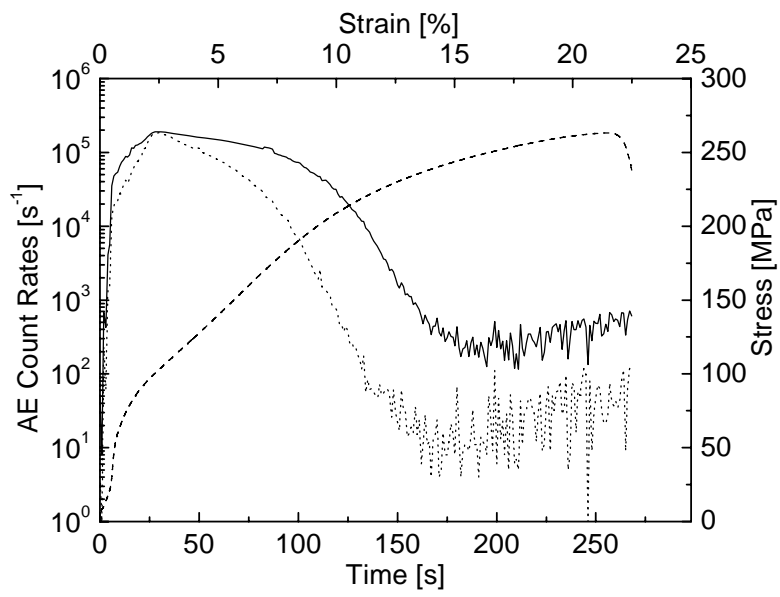


Fig 2c:

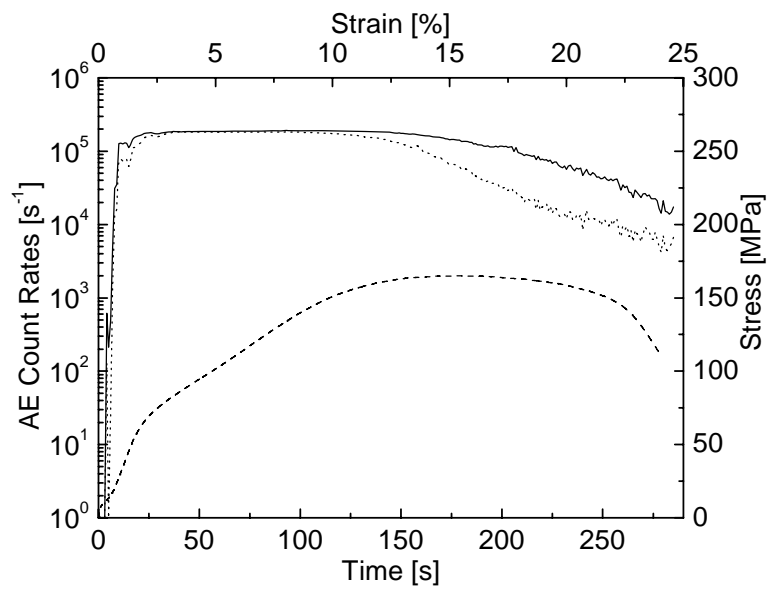


Fig 2d:

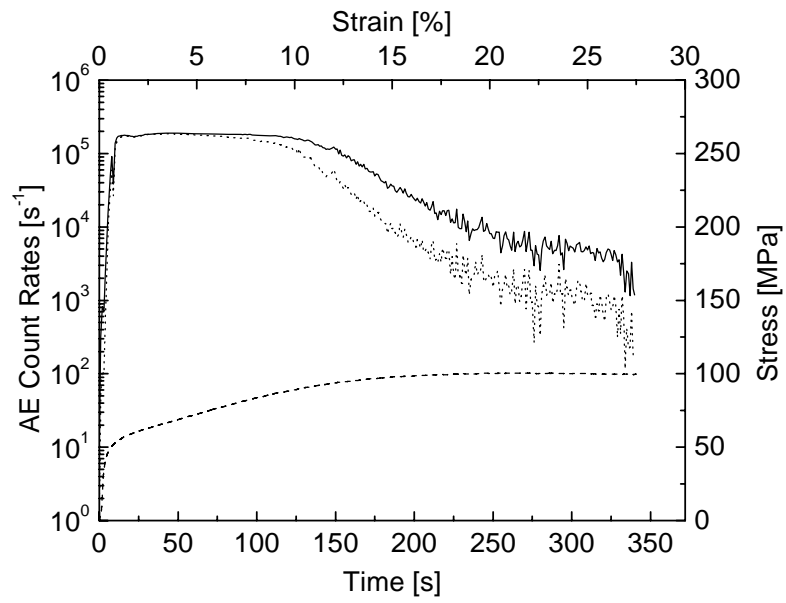


Fig 3a:

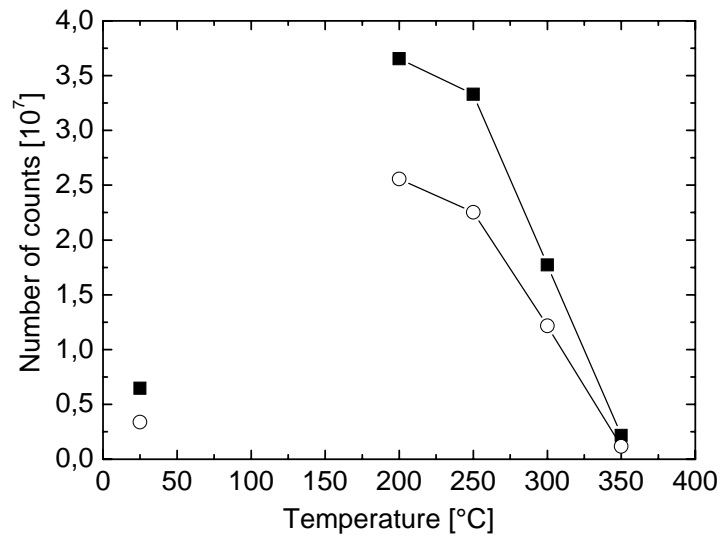


Fig 3b:

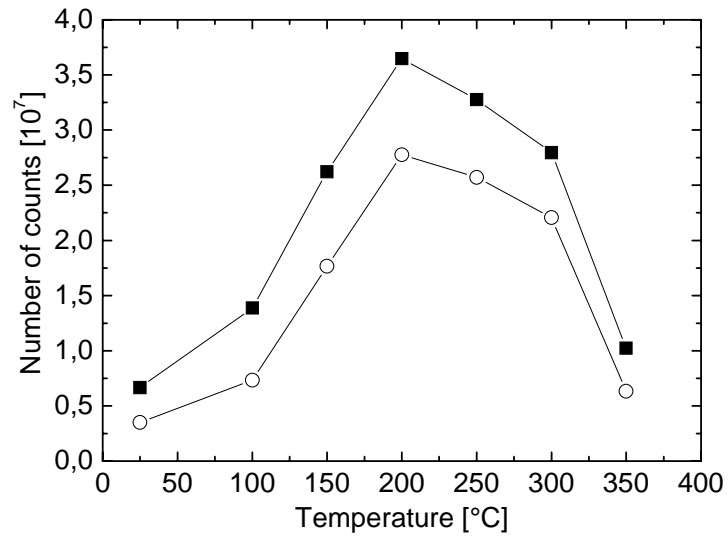


Fig 4:

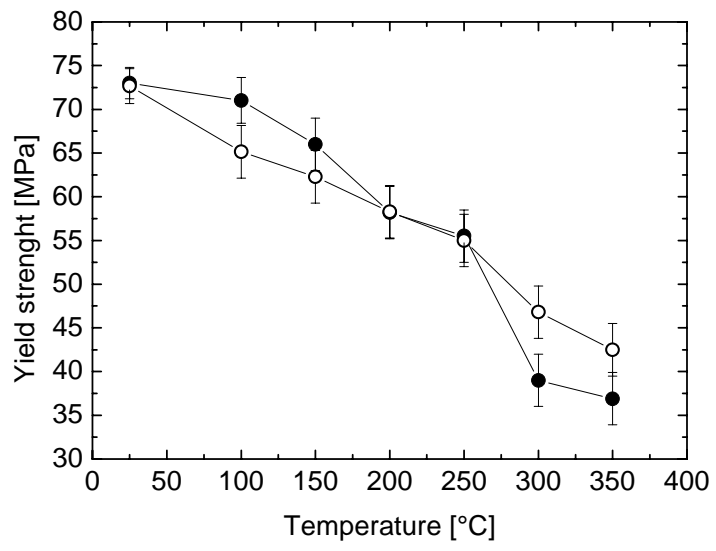


Fig 5a:

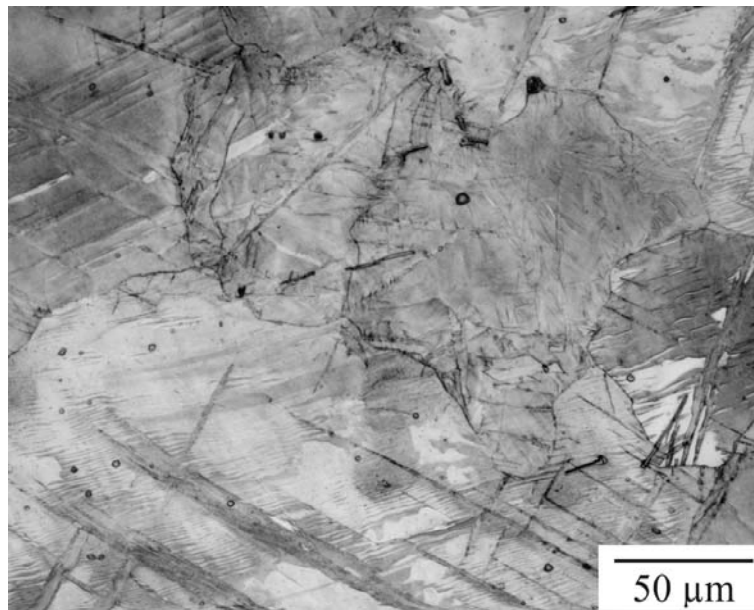


Fig 5b:

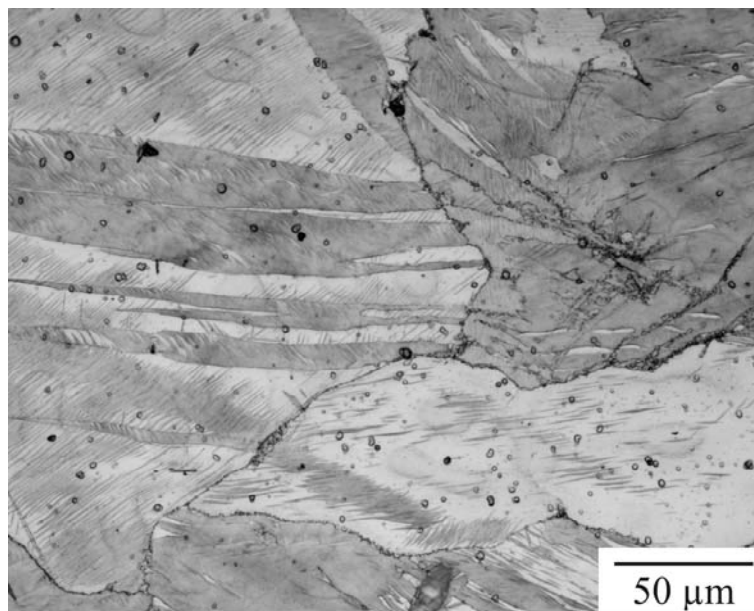


Fig 5c:

